Available online at www.worldnewsnaturalsciences.com

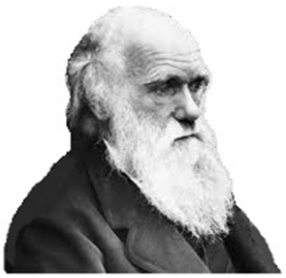

World News of Natural Sciences

An International Scientific Journal

WNOFNS 27 (2019) 22-37 EISSN 2543-5426

Adsorption behavior of pharmaceutically active dexketoprofen as sustainable corrosion Inhibitor for API X80 carbon steel in acidic medium

Nkem B. Iroha[1,*] and **Abosede O. James**[2]

[1]Electrochemistry and Material Science Unit, Department of Chemistry, Federal University, Otuoke, P.M.B 126, Yenagoa, Bayelsa, Nigeria

[2]Department of Pure and Industrial Chemistry, University of Port Harcourt, Port Harcourt, Nigeria

*E-mail address: irohanb@fuotuoke.edu.ng

ABSTRACT

The inhibition of X80 carbon steel corrosion in 1 M HCl solution by dexketoprofen (DKP) was studied using weight loss (WL), electrochemical impedance spectroscopy (EIS), potentiodynamic polarization (PDP) and scanning electron microscopy (SEM) techniques. The results indicated that DKP acts by way of adsorption as an effective protective inhibitor in the aggressive acid medium. The inhibition efficiency of DKP increased with concentration but was lower at higher temperature. The results of potentiodynamic polarization showed that DKP molecule behaved as a mixed type inhibitor by reducing both the anodic and the cathodic electrochemical reactions. Dexketoprofen was adsorbed on the X80 steel surface in accordance with Langmuir adsorption isotherm. SEM analyses supported formation of protective film on the X80 steel in the presence of DKP.

***Keywords*:** Dexketoprofen, Adsorption, Inhibition, Carbon steel, SEM

1. INTRODUCTION

Carbon steel is a material of choice, which has found wide application in many industries like petroleum, automobile, construction, metallurgical among others [1]. API X80 steel is a high strength carbon steel with high mechanical strength, good weldability and low hardenability, and thus is suitable for transporting different kinds of fluids under pressure, such

(Received 24 August 2019; Accepted 14 September 2019; Date of Publication 15 September 2019)

as oil and its derivatives. Corrosion is one of the major problems that pose a great danger to steel especially in the oil and gas industry. Industrial processes like acid pickling and oil well acidification typically use aggressive species, such as hydrochloric acid, which severely attacks carbon steel [2]. The practical solution of the problems of corrosion, lies in controlling it by reducing the rate at which the corrosion reactions proceed. Corrosion inhibitors are widely used in industry to reduce the corrosion rate of metals and alloys in contact with aggressive environment [3].

Organic compounds containing heteroatoms and aromatic rings are known to exhibit good inhibiting properties for steels in acidic environment [4-6]. It has been established that the common mechanism involved in any corrosion inhibition process is adsorption of the inhibitor on the metal surface [7, 8]. Adsorption of these compounds depends upon several factors including molecular weight, nature of substituents, solution temperature, nature of inhibitor and electrolytes etc. [9, 10]. Most efficient corrosion inhibitors available today are costly, poisonous, and constitute environmental hazards, hence the need for testing materials that are low cost and eco-friendly. Therefore, the current research is focused on the application of non-toxic eco-friendly corrosion inhibitor.

Nowadays, researchers have explored the potentials behind some drugs as green corrosion inhibitors for the corrosion of metals. On this list are clotrimazole [11], Rhodanine azosulpha [12], Norfloxacin and Sparfloxacin [13], Amoxicillin [14], methocarbamol [15], sulphadoxine and pyrimethamine [16], Trazodone [17], Tenormin [18], Fluconazole [19], Diclofenac sodium [20], among others. In all these and other studies, dexketoprofen has not been reported as an inhibitor for the corrosion of any metal in any medium. Dexketoprofen (DKP) is a nonsteroidal anti-inflammatory drug (NSAID). It prevents the production of prostaglandins and therefore reduces inflammation and pain. Along with peripheral analgesic action, it possesses central analgesic action. The objective of the present study is to investigate the adsorption and inhibitive properties of dexketoprofen for the corrosion of API X80 steel in 1 M HCl solution using weight loss (WL), electrochemical impedance spectroscopy (EIS), potentiodynamic polarization (PDP) and scanning electron microscopy (SEM) techniques.

2. MATERIALS AND METHODS

2. 1. Materials

Carbon sheets of type API 5L X80 having weight percentage composition of C-0.065%, Si-0.29%, Mn-1.5%, P-0.015%, Al-0.003%, Mo-0.28% Ti-0.020%, Nb-0.076% and the remainder being iron were used for gravimetric, surface analysis and the electrochemical measurements. The sheets were mechanically press-cut into coupons having dimension 2 cm × 2 cm for weight loss and surface analysis and 1 cm × 1 cm for electrochemical measurements and containing a small hole of about 0.10 mm diameter near the upper edge. The X80 steel coupons were abraded with 600 - 1000 grade silicon carbide papers, washed by double distilled water, degreased with acetone, dried at room temperature and stored in a moisture-free desiccator before their use in corrosion studies.

The acid solution of 1 M HCl was prepared by dilution of analytical grade 37% HCl with double distilled water. Dexketoprofen (DKP) manufactured by Menarini and marketed under the trade name Ketesse was purchased from Sabheik Pharmaceuticals Nig. Ltd., and used for corrosion testing without further purification. The molecular formula of the drug is $C_{16}H_{14}O_3$

and its molecular and optimized structures are shown in Scheme 1. Different amounts of DKP were dissolved in 1 M HCl solution to prepare the desired concentrations in ppm.

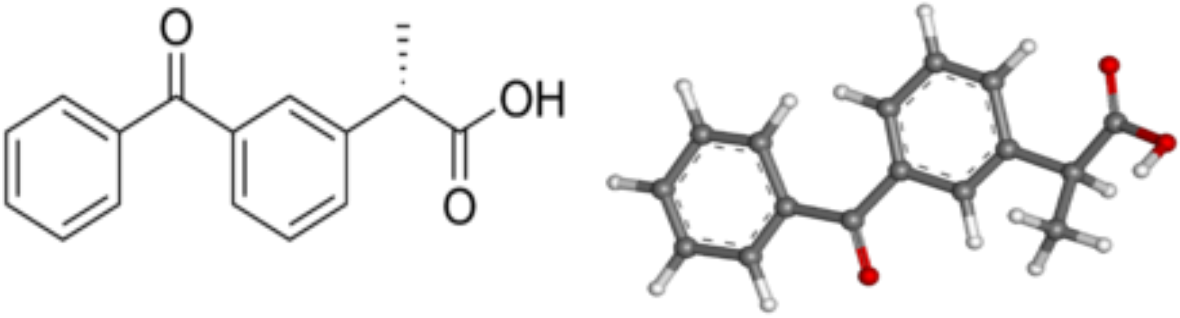

(a) **(b)**

Scheme 1. Structure of (2S)-2-[3-(benzoyl)phenyl]propanoic acid (Dexketoprofen)
(a) Molecular structure **(b)** Optimized structure: O - red; C - gray; H - white.

2. 2. Weight loss measurements

The X80 steel coupons were initially weighed in an electronic balance. After that the coupons were immersed for in 1 M HCl solutions without and with different concentrations of the DKP maintained at 30, 40 and 50 °C respectively, in a water bath.

The specimens were removed after 24 h exposure period at, washed with water to remove any corrosion product, rinsed with acetone, dried and reweighed to determine the weight loss. The tests were performed in triplicate to guarantee the reliability of the results and the mean value of the weight loss is reported. The weight loss values were used to calculate the mean corrosion rate in ($mg \cdot cm^{-2}$).

The corrosion rate of mild steel was determined using the relation [21]:

$$CR = \frac{\Delta W}{At} \tag{1}$$

where: ΔW is the weight loss, A is the area and t is the immersion period. The surface coverage (θ) and percentage inhibition efficiency (η_{WL} (%)) were calculated from the corrosion rate data according to equations 2 and 3, respectively [22].

$$\theta = \left(1 - \frac{CR_{inh}}{CR_{bla}}\right) \tag{2}$$

$$\eta_{WL}(\%) = \theta(1000) \tag{3}$$

where: CR_{bla} and CR_{inh} are the corrosion rates of X80 steel in the absence and presence of inhibitor, respectively.

2. 3. Electrochemical measurements

The electrochemical experiments were performed using Parstat 2263 potentiostat at 30 ºC. A standard three electrode cell assembly was used for this purpose. It consisted of the API X80 carbon steel specimen as working electrode (1 cm^2), a platinum foil as a counter electrode and saturated calomel electrode (SCE) as a reference electrode. A luggin capillary arrangement was used to keep the SCE close to the working electrode to avoid the ohmic contribution. A stabilization period of 30 minutes was allowed for potentiodynamic polarization (PDP) and electrochemical impedance spectroscopy (EIS) experiments. PDP runs were conducted in the potential range from -250 mV to +250 mV relative to the corrosion potential. A scan rate of 1 mVs^{-1} was used for the PDP runs. The Tafel extrapolation method was used in the calculation of corrosion current densities and other Tafel fit parameters. All potential values were reported versus SCE. EIS runs were performed in the frequency range of 100 kHz to 100 mHz at an amplitude of 10 mV. The impedance measurements were conducted at open circuit potential (OCP). All the measurements were done in solutions open to air under unstirred conditions.

2. 4. Surface analysis

The scanning electron microscope (SEM) model FEG 250 was used to examine the X80 steel surface after immersion in corrosive media in the absence and presence of dexketoprofen (DKP) for 24 h. The X80 steel surfaces pretreated as described in Section 2.1 were immersed in 1 M HCl solution without and with 500 ppm concentration of DKP. After 24 h, the specimens were retrieved, washed with water, dried and used for SEM analysis.

3. RESULTS AND DISCUSSION

3. 1. Weight loss method

The variation of corrosion rate with DKP concentration for X80 steel corrosion in 1 M HCl without and with different concentrations of dexketoprofen (DKP) at 303, 313 and 323 K, respectively is presented in Figure 1. From the graph, it was observed that the corrosion rate of X80 steel in the acid decreases with increasing concentration of the inhibitor but increases with increasing temperature. This behavior reflects the inhibitory effect of DKP toward the acid corrosion of the steel and that the extent of corrosion inhibition is dependent on the concentration of the inhibitor. This is probably due to the fact that the surface coverage of the steel increases by the adsorption of inhibitor molecules.

Plot of the inhibition efficiency η_{WL} (%) versus inhibitor concentration is shown in Figure 2. From the figure, it could be observed that the values of η_{WL} were gradually increased with the increase in concentration of DKP, reaching a maximum value of 94.23 % at the highest concentration of 1000 ppm at temperature of 303 K. Several researchers in their studies reported similar results for green inhibitors [23-27].

However, the inhibition efficiency decreases with temperature rise which could be due to the desorption effect of the inhibitor molecules. Decrease in inhibition efficiency with increase in temperature indicates and that the adsorption of the inhibitor favours the mechanism of physical adsorption.

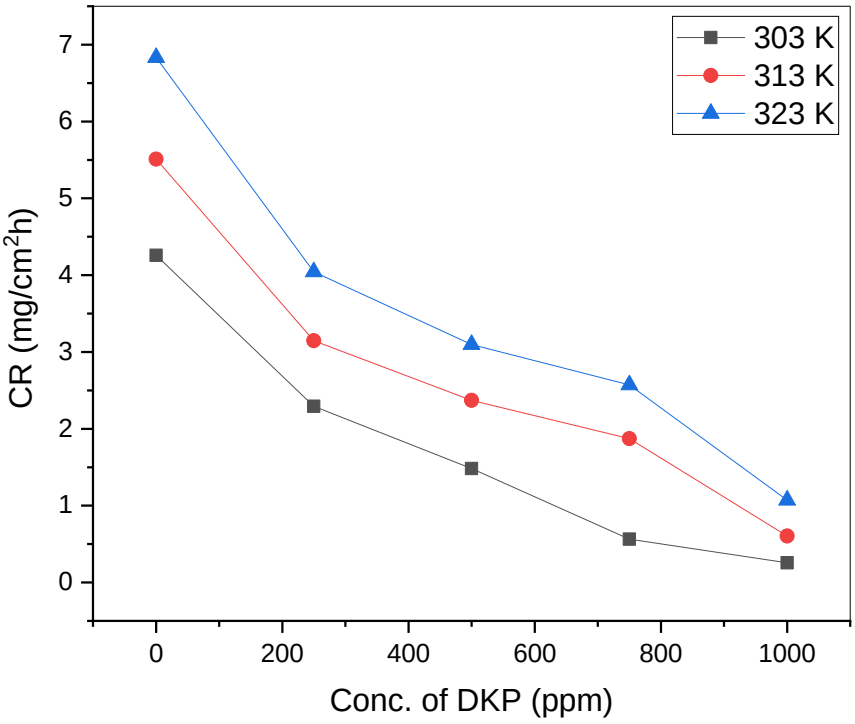

Figure 1. Variation of corrosion rate with inhibitor concentration for X80 steel corrosion in 1 M HCl without and with different concentrations of DKP at different temperatures.

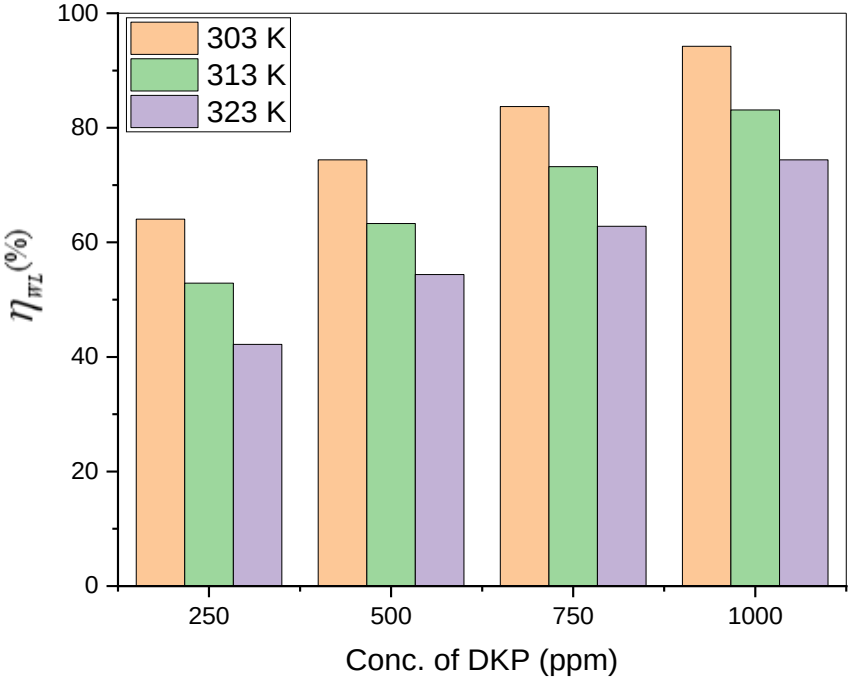

Figure 2. Variation of η_{WL} (%) with inhibitor concentration for X80 steel corrosion in 1 M HCl without and with different concentrations of DKP at different temperatures.

3. 2. Electrochemical impedance spectroscopy

The Electrochemical impedance spectroscopy (EIS) measurements were performed on X80 steel in 1 M HCl without and with different concentrations of dexketoprofen (DKP). Figures 3 shows Nyquist plots obtained from the EIS measurements at 303 K. The impedance spectra in the absence and presence of DKP exhibit one single depressed semicircular capacitive loop, which may be attributed to the charge transfer reaction and suggesting that the studied inhibitor is controlling the corrosion reaction without modifying the mechanism of X80 steel [28]. The depression in semicircle loop is usually attributed to the roughness and other inhomogeneities of the solid electrode [29].

Furthermore, the diameter of the capacitive loop in the presence of inhibitor is larger than that in the blank acid solution, and increased with the inhibitor concentration. Impedance data were analyzed using the equivalent circuit as shown in Figure 4, which consist of the solution resistance (R_s) in series with the parallel combination of constant phase element (CPE) in place of double layer capacitance (C_{dl}) and charge transfer resistance (R_{ct}). Mathematically, the impedance of the CPE is given by:

$$Z_{CPE} = Y_o^{-1}(j\omega)^{-n} \tag{4}$$

where: Y_o is the CPE constant, j is the imaginary unit ($j^2 = -1$), ω is the angular frequency ($\omega = 2\pi f$, f is the frequency in Hz), and n is the CPE exponent also known as the phase shift which is related to the degree of surface inhomogeneity. The value of C_{dl} was obtained from the following equation:

$$C_{dl} = Y_o(2\pi f_{\max})^{n-1} \tag{5}$$

where: f_{max} is the frequency at which the imaginary part of impedance is maximum. The inhibition efficiency was calculated using following equation [30]:

$$\eta_{EIS}(\%) = \left[\frac{R_{ct}^{inh} - R_{ct}^{bla}}{R_{ct}^{inh}}\right]100 \tag{6}$$

where: R_{ct}^{bla} and R_{ct}^{inh} are charge transfer resistances in absence and presence of DKP respectively. The derived impedance parameters along with the inhibition efficiency η_{EIS} (%) are listed in Table 1.

The results in Table 1 show that the R_{ct} values increase with increasing concentration of DKP and the C_{dl} values for the inhibited solutions are generally lower than that of the acid blank, which suggest that the inhibitor adsorb on the steel surface thereby forming a protective layer on the steel surface and reducing the rate of charge transfer process.

Agian, it is clearly seen that the inhibition efficiency in 1 M HCl solution increases with the increase in the concentration of dexketoprofen (DKP). The results show that the inhibition efficiencies obtained from the impedance study are in good agreement with those from the previous gravimetric measurements.

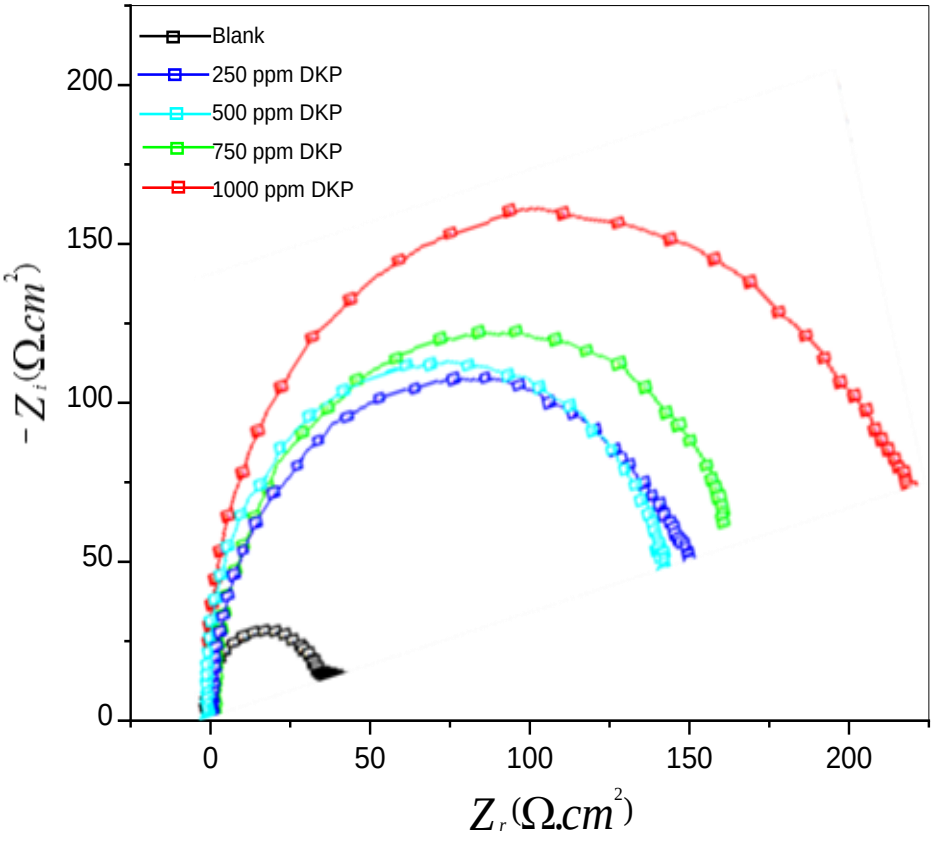

Figure 3. Nyquist plots recorded for X80 steel in 1M HCl in the absence and presence of different concentrations of DKP

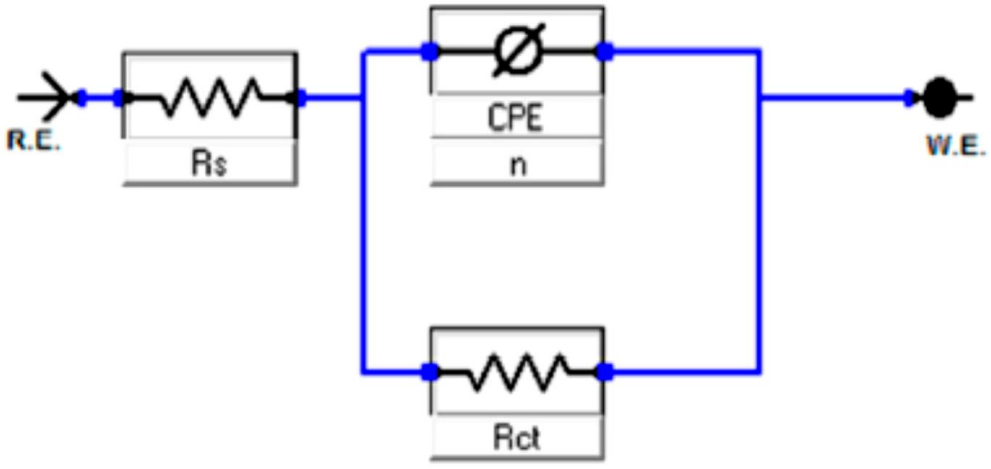

Figure 4. Equivalent circuit used to model the impedance data of X80 steel in the absence and presence of different concentrations of DKP at 303 K.

Table 1. Impedance parameters obtained from Nyquist plots for X80 steel in 1 M HCl at different concentrations of DKP.

DKP Conc. (ppm)	R_s (Ω cm^2)	R_{ct} (Ω cm^2)	Y_o ($\mu\Omega^{-1}s^2cm^{-2}$)	C_{dl} (μFcm^{-2})	n	η_{EIS} (%)
0	1.009	20.6	264.8	189.4	0.901	
250	1.271	50.4	229.9	95.3	0.917	59.1
500	1.398	80.9	205.8	77.4	0.923	74.5
750	1.521	119.3	214.3	52.9	0.911	82.7
1000	1.700	134.7	193.7	39.6	0.918	84.7

3. 3. Polarization measurements

The potentiodynamic polarization curves for API X80 carbon steel in the absence and presence of various concentrations of dexketoprofen (DKP) in 1 M HCl solution are shown in Figure 5. The polarization parameters such as corrosion potential (E_{corr}), corrosion current density (I_{corr}), anodic Tafel slope (β_a) and cathodic Tafel slope (β_c) were deduced by extrapolating the linear branches of the anodic Tafel slopes and displayed in Table 2.

The corrosion inhibition efficiency was calculated using Equation 7 [31] and also displayed in Table 2.

$$\eta_{PDP}(\%) = 100\left(\frac{I_{corr}^{bla} - I_{corr}^{inh}}{I_{corr}^{bla}}\right) \quad (7)$$

where: I_{corr}^{bla} and I_{corr}^{inh} represent the corrosion current densities with and without inhibitor respectively.

Table 2. Polarization parameters for X80 steel corrosion in 1 M HCl without and with different concentrations of DKP

DKP Conc. (ppm)	E_{corr} (mV/SCE)	β_c (mV/dec)	β_a (mV/dec)	I_{corr} (mA/cm^2)	η_{PDP} (%)
0	-498	187.3	97.9	1288.6	-
250	-471	201.9	131.4	351.8	72.7
500	-465	226.8	149.1	299.5	76.7
750	-450	198.0	158.5	164.7	87.2
1000	-446	234.7	155.2	122.0	90.5

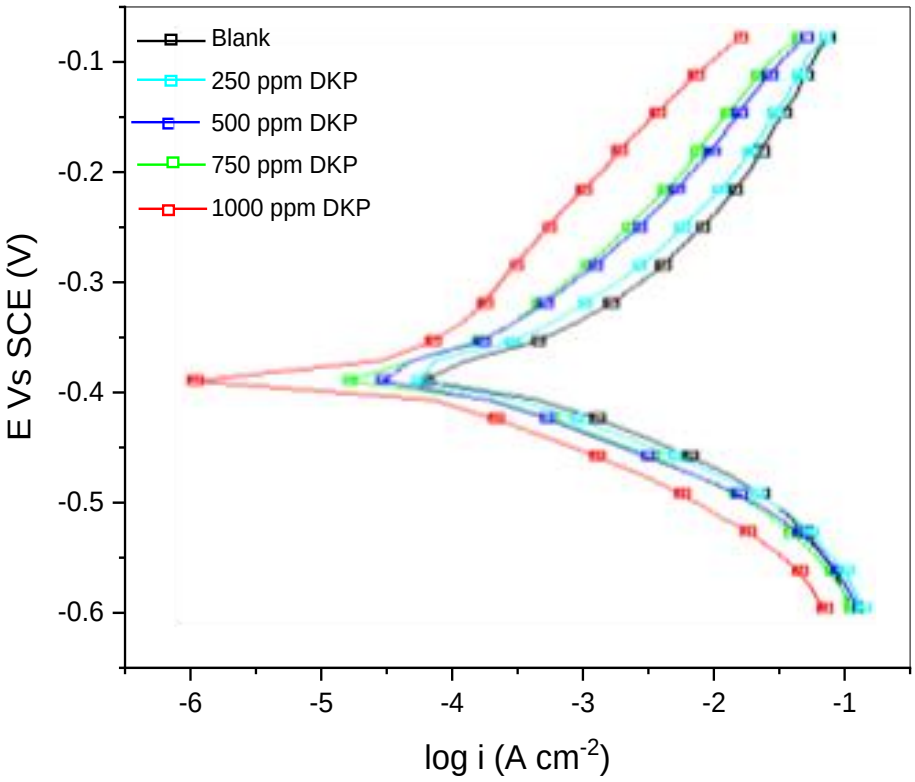

Figure 5. Potentiodynamic polarization curves for X80 steel in 1 M HCl without and with various concentrations of DKP

It can be observed from Figure 5 and Table 2 that the introduction of DKP to the 1 M HCl solution brings about a significant suppression of the corrosion current density reflecting the inhibition of the X80 steel corrosion reactions. In addition, the cathodic and anodic arms of the polarization curves are both shifted towards lower values in the presence of the DKP, suggesting that DKP reduced the rate of anodic X80 steel dissolution in the acid as well as the cathodic hydrogen ion reduction. The extent of the shift in E_{corr} in the presence of the DKP compared to the blank is generally less than 85 mV, suggesting that the DKP act as mixed-type inhibitors [32-34]. The change in the values of β_a and β_c at different concentrations of the inhibitor can be attributed to the occurrence of redox complexation reactions of Fe-inhibitor complexes involving different oxidation states of Fe in the electrochemical systems [35]. Table 2 clearly shows that as the concentrations of DKP increases, there is an increase in the corrosion inhibition efficiency due to the adsorption of inhibitor on the steel surface.

3. 4. Adsorption isotherm

Adsorption of a corrosion inhibitor on metal surface can occur through physisorption or chemisorption mechanism or a competitive form of both mechanisms. The adsorption of the inhibitor (DKP) molecules was investigated by different adsorption isotherm models such as Langmuir, Frumkin and Temkin. Out of these isotherms, Langmuir model showed the best fit and is expressed by the following equation [25]:

$$\frac{C}{\theta} = \frac{1}{K_{ads}} + C \tag{8}$$

where, K_{ads} is equilibrium adsorption constant, C is inhibitor concentration and θ is the fraction of surface covered by inhibitor. The plots C/θ against C for X80 steel in 1 M HCl solution at different temperatures are shown in Figure 6. The values of K_{ads} were calculated from the intercepts of the straight lines on the C/θ. It is a known fact that K_{ads} represents the strength of adsorption or desorption between adsorbate and adsorbent. Large values of K_{ads} correspond to more efficient adsorption. The slight deviations of the slopes of the Langmuir plots from unity are due to the interactions between the adsorbed molecules on the metal surface as well as change in the heat of adsorption with increasing surface coverage [36]. The adsorption equilibrium constant, K_{ads} is related to the change in Gibbs free energy of adsorption (ΔG_{ads}) as:

$$\Delta G^{o}_{ads} = -RT\ln(55.5K_{ads}) \tag{9}$$

where: R is the gas constant (8.314 J K^{-1} mol^{-1}), T is the absolute temperature and 55.5 is the concentration of water solution. Thermodynamic parameters for the adsorption process obtained from Langmuir adsorption isotherm are given in Table 3. K_{ads} values decrease with increase in temperature indicating decrease in adsorption strength, probably due to desorption of DKP molecules.

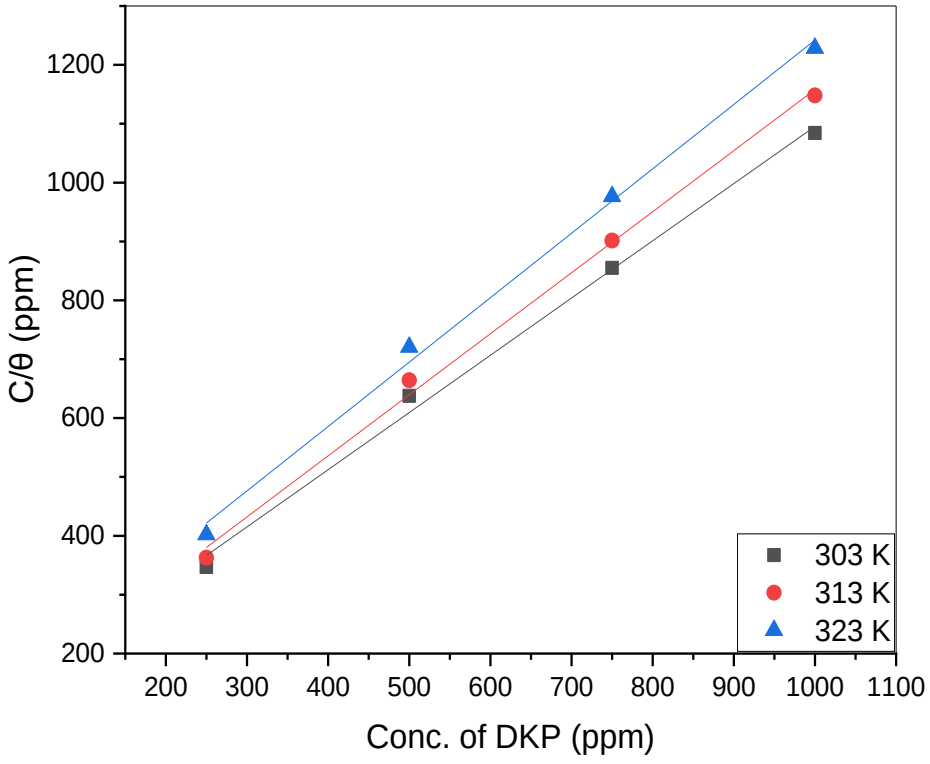

Figure 6. Langmuir isotherm for the adsorption of DKP on X80 steel surface at different temperatures

The negative values of $\Delta G°_{ads}$ implies spontaneity of the adsorption process and stability of the adsorbed film on the X80 steel surface. Generally, the values of $\Delta G°_{ads}$ up to -20 kJmol^{-1} are attributed to physisorption while those around -40 kJmol^{-1} or more negative are associated with chemisorption process [37]. The $\Delta G°_{ads}$ values obtained in this study are between -39.8 kJ mol^{-1} and -26.6 kJ mol^{-1} which imply that adsorption involves physisorption.

Table 3. Langmuir parameters for the adsorption of DKP on X80 steel surface at different temperatures

Temperature (K)	Slope	K_{ads}	R^2	ΔG^o_{ads} (kJmol^{-1})
303	0.9717	0.0958	0.9934	-4.21
313	1.0369	0.0810	0.9955	-3.91
323	1.0942	0.0687	0.9949	-3.59

3. 5. Effect of temperature

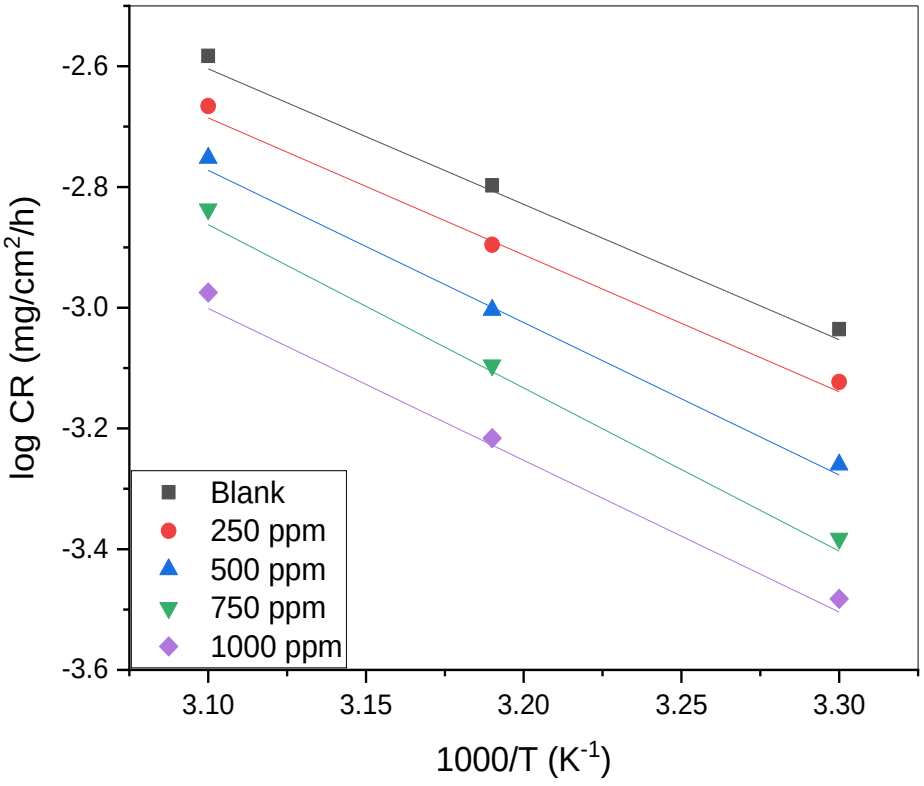

Figure 7. Arrhenius plot for DKP adsorption on X80 steel in 1 M HCl solution

The effect of temperature was studied using the weight loss experiments in the absence and presence of various concentrations of DKP for 24 h immersion time in the temperature range of 303-323 K. From the results depicted in Figure 1 and 2 and already discussed in section 3.1, it is seen that an increase in temperature causes significant decrease in the η_{WL} and increase in the CR. The effect of temperature on the inhibition efficiency of DKP can be explain with the aid of Arrhenius equation presented bellows [38]:

$$\log CR = \frac{-E_a}{2.303RT} + \log A \qquad (10)$$

where: CR , R, T and A denote the corrosion rate, the universal gas constant, the absolute temperature and Arrhenius pre-exponential factor, respectively. E_a represents the activation energy and its values for corrosion of inhibited and non-inhibited X80 steel were derived from the slopes of Arrhenius plots shown in Figure 7.

The E_a values for X80 steel in 1 M HCl in the absence of DKP is 35.61 kJ mol^{-1} and in the presence of 250, 500, 750 and 1000 ppm concentrations of DKP were 42.90 kJ mol^{-1}, 48.15 kJ mol^{-1}, 51.84 kJ mol^{-1} and 56.31 kJ mol^{-1}. An increase in activation energy is observed as the DKP concentration increases.

The higher values of E_a for inhibited cases as compared to uninhibited case indicate that in the presence of DKP X80 steel corrosion became difficult owing to the adsorption of the molecules of DKP on the metallic surface [39].

3. 6. Surface analysis

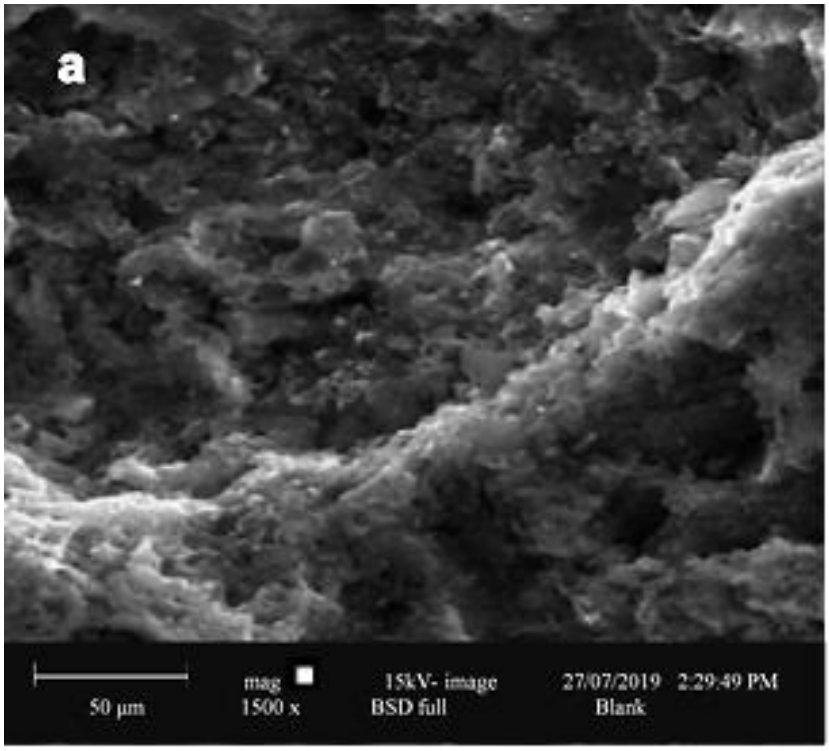

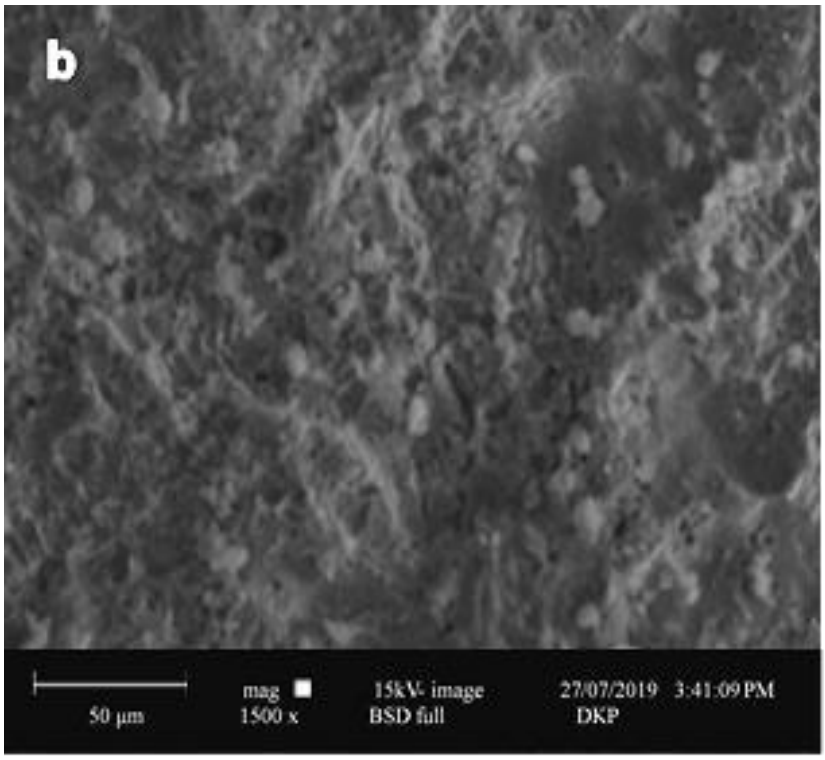

Figure 8. SEM micrographs of X80 steel corrosion in **(a)** uninhibited 1 M HCl solution and **(b)** 1 M HCl solution+1000 ppm of DKP at 303K

The SEM images of X80 steel specimens in 1 M HCl without and with 1000 ppm of the dexketoprofen (DKP) are presented in Figure 8. It can be seen that X80 steel surface in the absence of inhibitor (Figure 8(a)) appears very rough with clearly observed cavity and pits. That means that, X80 steel surface is highly damaged in the absence of DKP.

The X80 steel specimen retrieved from the acid solution containing 1000 ppm DKP (Figure 8(b)) generally show less damaged surface with minor pits and cracks which confirms that the DKP molecules form protective films on the steel surface thereby reducing the corrosion process.

4. CONCLUSIONS

Dexketoprofen (DKP) was investigated as corrosion inhibitor for X80 carbon steel in 1 M HCl solution. DKP inhibited the corrosion of the steel with the inhibition efficiency increasing with increasing concentration of inhibitor but decreases on rise in temperature.

Potentiodynamic polarization measurements revealed that DKP acted as a mixed type corrosion inhibitor. Impedance measurements revealed that DKP form protective film on X80 steel surface thereby reducing the rate of charge transfer process. The adsorption behaviour of DKP on X80 steel surface in 1 M HCl obeys the Langmuir adsorption isotherm and involves physical adsorption mechanism. SEM images confirmed the formation of protective film by DKP on X60 steel surface.

References

[1] H. F. El-Shamy, Y. A. Aggour, A. M. Ahmed, Study the metallic finishing and corrosion control processes for carbon steel overhead pipes using polymer molecules. *MOJ Biorg Org Chem* 1(5) (2017) 1-11

[2] K. Zhang, B. Xu, W. Yang, X. Yin, Y. Liu, Y. Chen, Halogen-substituted imidazoline derivatives as corrosion inhibitors for mild steel in hydrochloric acid solution. *Corros. Sci.* 90 (2015) 284-295.

[3] X. Zheng, S. Zhang, W. Li, L. Yin, J. He, J. Wu, Investigation of 1-butyl-3-methyl-1H-benzimidazolium iodide as inhibitor for mild steel in sulfuric acid solution. *Corros Sci*. 80 (2014) 383-392

[4] A. Alobaidy, A. Kadhum, S. Al-Baghdadi, A. A. Al-Amiery, E. Yousif, A. Mohamad, Eco-Friendly Corrosion Inhibitor: Experimental Studies on the Corrosion Inhibition Performance of Creatinine for Mild Steel in HCl Complemented with Quantum Chemical Calculations. *Int. J. Electrochem. Sci.* 10 (2015) 3961-3972

[5] E. Yousif, Y. Win, A. H. Al-Hamadani, A. A. Al-Amiery, A. Mohamad, Furosemide as an Environmental-Friendly Inhibitor of Corrosion of Zinc metal in Acid Medium: Experimental and Theoretical studies. *Int. J. Electrochem. Sci.* 10 (2015) 1708-1715

[6] N. B. Iroha, E. E. Oguzie, G. N. Onuoha and A. I. Onuchukwu, Inhibition of Mild Steel Corrosion in Acidic Solution by derivatives of Diphenyl Glyoxal. *16th International Corrosion Congress, Beijing, China*, (20051) 26-131

[7] H. Ashassi-Sorkhabi, B. Shaabani, D. Seifzadeh, Effect of Some Pyrimidinic Shciff Bases on the Corrosion of Mild Steel in Hydrochloric Acid Solution. *Electrochim. Acta* 50 (2005) 3446-3452

[8] N. O. Eddy, S. A. Odoemelam, A. O. Odiongenyi, Joint effect of halides and ethanol extract of *Lasianthera africana* on inhibition of corrosion of mild steel in H_2SO_4. *J. Appl. Electrochem.* 39 (2009) 849-857

[9] A. Barbosa da Silva, E. D'Elia, J. A. C. P. Gomes, Carbon steel corrosion inhibition in hydrochloric acid solution using a reduced Schiff base of ethylenediamine. *Corros. Sci.* 52 (2010) 788-793

[10] C. Verma, M. A. Quraishi, A. Singh, 5-Substituted 1H-tetrazoles as effective corrosion inhibitors for mild steel in 1 M hydrochloric acid. *J. Taibah Uni. Sci.* 10 (2016) 718-733

[11] I. B. Obot, N. O. Obi-Egbedi, S. A. Umoren, Adsorption characteristics and corrosion inhibitive properties of clotrimazole for aluminium corrosion in hydrochloric acid. *International Journal of Electrochemical Science* 4 (2009) 863- 877

[12] M. Abdallah, Rhodanine azosulpha drugs as corrosion inhibitors for corrosion of 304 stainless steel in hydrochloric acid solution. *Corrosion Science* 44 (2002) 717-728

[13] N. O. Eddy, S. A. Odoemelam, Norfloxacin and Sparfloxacin as corrosion inhibitors for zinc. Effect of concentrations and temperature. *Journal of Materials Science* 4 (2008) 87-96

[14] A. S. Mahdi, Amoxicillin as green corrosion inhibitor for concrete reinforced steel in simulated concrete pore solution containing chloride. *International Journal of Advanced Research in Engineering and Technology* 5 (2014) 99-107

[15] E. E. Ebenso, N. O. Eddy, A. O. Odiongenyi, Corrosion inhibition and adsorption properties of methocarbamol in mild steel in acidic medium. *Portugaliae Electrochimica Acta* 27 (2009) 13-22

[16] I. A. Akpan, N. O. Offiong, Electrochemical study of corrosion inhibition action of sulphadoxine and pyrimethamine on mild steel in acidic medium. *International Journal of Chemical and Process Engineering Research* 1 (2014) 10-18

[17] S. Mani megalai, R. Ramesh, P. Manjula, Inhibition of corrosion mild steel in acid media by Trazodone drug. *Research Desk* 2 (2013) 326-333

[18] A. S. Fouda, S. M. Rashwan, M. M. Kamel, A. Ibrahim, Tenormin drug as save corrosion inhibitor for 304 stainless steel in hydrochloric acid solutions. *Der Pharma Chemica* 7 (2015) 22-33

[19] P. M. Nouri, M. M.Attar, Experimental and quantum chemical studies on corrosion inhibition performance of Fluconazole in hydrochloric acid solution. *Bulletin of Materials Science* 38 (2015) 499-509

[20] K. R. Ansari, M. A. Quraishi, E.E. Ebenso, Electrochemical and thermodynamic investigation of Diclofenac sodium drug as a potential corrosion inhibitor for mild steel in hydrochloric acid. *International Journal of Electrochemical Science* 8 (2013) 12860-12873

[21] N. B. Iroha and A. Hamilton-Amachree, Adsorption and anticorrosion performance of Ocimum Canum extract on mild steel in sulphuric acid pickling environment. *American Journal of Materials Science* 8(2) (2018) 39-44.

[22] N. A. Madueke and N. B. Iroha, Protecting aluminium alloy of type AA8011 from acid corrosion using extract from Allamanda cathartica leaves. *International Journal of Innovative Research in Science, Engineering and Technology* 7(10) (2018) 10251-10258

[23] O. James and E. O. Ekpe, Inhibition of corrosion of mild steel in 2M hydrochloric acid by Aloe Vera. *International Journal of Pure and Applied Chemistry* 35(10) (2002)

[24] J. N. O. Ezeugo, O. D. Onukwuli, M. Omotioma. Optimization of corrosion inhibition of Picralima nitida leaves extract as green corrosion inhibitor for zinc in 1.0 M HCl. *World News of Natural Sciences* 15 (2017) 139-161

[25] N. B. Iroha and A. O. James, Assessment of performance of velvet tamarind-furfural resin as corrosion inhibitor for mild steel in acidic solution. *J. Chem Soc. Nigeria* 43(3) (2018) 510-517

[26] H. Louis, J. Japari, A. Sadia, M. Philip, A. Bamanga. Photochemical screening and corrosion inhibition of Poupartia birrea back extracts as a potential green inhibitor for mild steel in 0.5 M H2SO4 medium. *World News of Natural Sciences* 10 (2017) 95-100

[27] N. B. Iroha, O. Akaranta and A. O. James, Corrosion Inhibition of Mild Steel in Acid Media by Red Peanut skin extract-furfural Resin. *Advances in Applied Science Research* 3(6) (2012) 3593-3598

[28] S. A. Umoren, Y. Li, F. H. Wang, Electrochemical study of corrosion inhibition and adsorption behaviour for pure iron by polyacrylamide in H_2SO_4: Synergistic effect of iodide ions. *Corros. Sci.* 52 (2010) 1777-1786

[29] M. Scendo, J. Uznanska, The effect of ionic liquids on the corrosion inhibition of copper in acidic chloride solutions. *Int J Corros* (2011) 1-13

[30] N. B. Iroha, A. Hamilton-Amachree, Inhibition and adsorption of oil extract of Balanites aegyptiaca seeds on the corrosion of mild steel in hydrochloric acid environment. *World Scientific News* 126 (2019) 183-197.

[31] A. O. James and N. B. Iroha, An Investigation on the Inhibitory Action of Modified Almond Extract on the Corrosion of Q235 Mild Steel in Acid Environment, *IOSR Journal of Applied Chemistry* 12(2) (2019) 01-10

[32] E. S. Ferreira, C. Giancomelli, F. C. Giacomelli, A. Spinelli, Evaluation of the inhibitor effect of l-ascorbic acid on the corrosion of mild steel. *Mater. Chem. Phys.* 83 (2004) 129-134

[33] H. A. Sorkhabi, M. R. Majidi, K. Seyyedi, Investigation of inhibition effect of some amino acids against steel corrosion in HCl solution. *Appl. Surf. Sci.* 225 (2004) 176-185

[34] [34] M. A. Chidiebere, N. Simeon, D. Njoku, N. B. Iroha, E. E. Oguzie and Y. Li, Experimental study on the inhibitive effect of phytic acid as a corrosion inhibitor for Q235 mild steel in 1 M HCl environment. *World News of Natural Sciences* 15 (2017) 1-19

[35] L. O. Olasunkanmi, M. M. Kabanda, E. E. Ebenso, Quinoxaline derivatives as corrosion inhibitors for mild steel in hydrochloric acid medium: Electrochemical and quantum chemical studies. *Physica E* 76 (2016) 109-126

[36] A. Bouyanzer, B. Hammouti, L. Majidi, Pennyroyal oil from Mentha pulegium as corrosion inhibitor for steel in 1 M HCl. *Materials Letters* 60(23) (2006) 2840-2843

[37] N. B. Iroha and M. A. Chidiebere, Evaluation of the Inhibitive Effect of Annona Muricata. L Leaves Extract on Low-Carbon Steel Corrosion in Acidic Media. *International Journal of Materials and Chemistry* 7(3) (2017) 47-54

[38] C. Verma, L. O. Olasunkanmi, E. E. Ebenso, M. A. Quraishi, I. B. Obot, Adsorption behavior of glucosamine-based, pyrimidine-fused heterocycles as green corrosion inhibitors for mild steel: experimental and theoretical studies. *J. Phys. Chem. C* 120 (2016) 11598-11611.

[39] Z. Z. Tong, J. Q. Xue, R. Y. Wang, J. Huang, J. T. Xu, Z. Q. Fan, Hierarchical self-assembly, photo-responsive phase behavior and variable tensile property of azobenzene-containing ABA triblock copolymers. *RSC Adv.* 5 (2015) 4030-4040